

# Separators in Enhancing Autoregressive Pretraining for Vision Mamba

Hanpeng Liu

Zidan Wang

Shuoxi Zhang

Kaiyuan Gao

Kun He\*

Huazhong University of Science and Technology

brooklet60@hust.edu.cn

## Abstract

The state space model Mamba has recently emerged as a promising paradigm in computer vision, attracting significant attention due to its efficient processing of long sequence tasks. Mamba’s inherent causal mechanism renders it particularly suitable for autoregressive pretraining. However, current autoregressive pretraining methods are constrained to short sequence tasks, failing to fully exploit Mamba’s prowess in handling extended sequences. To address this limitation, we introduce an innovative autoregressive pretraining method for Vision Mamba that substantially extends the input sequence length. We introduce new *Separators* for *AutoRegressive* pretraining to demarcate and differentiate between different images, known as *STAR*. Specifically, we insert identical separators before each image to demarcate its inception. This strategy enables us to quadruple the input sequence length of Vision Mamba while preserving the original dimensions of the dataset images. Employing this long sequence pretraining technique, our *STAR-B* model achieved an impressive accuracy of 83.5% on ImageNet-1k, which is highly competitive in Vision Mamba. These results underscore the potential of our method in enhancing the performance of vision models through improved leveraging of long-range dependencies.

## 1. Introduction

Recent advancements in state space models [14] have significantly impacted the field of deep learning, particularly within natural language processing. Mamba [10], a novel variant in this domain, has surpassed traditional state space models by integrating the best attributes of selective scanning. Its linear complexity and selective scanning mechanisms have resulted in impressive computational efficiency when processing long contexts. This advantage has accelerated the deployment of Mamba across various visual tasks, spurring the rapid emergence and application of Vi-

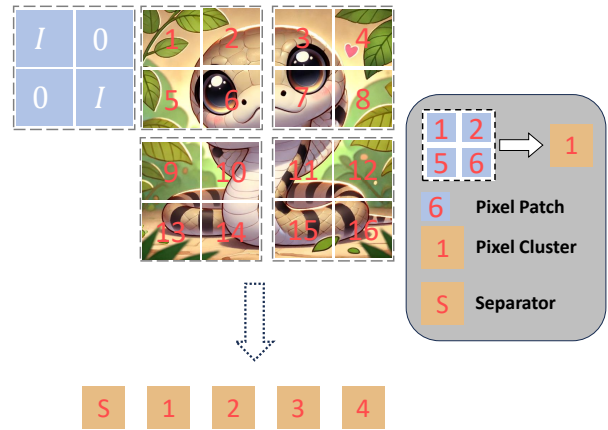


Figure 1. Each image is divided into non-overlapping patches. Multiple spatially adjacent patches are grouped into a cluster. Our STAR adds a separator at the beginning of each image. This separator is also a cluster, with patches on its internal diagonal being vector  $\mathbf{1}$ , and other positions being vector  $\mathbf{0}$ .

sion Mamba models in areas such as image classification [26, 35], object detection [16, 33], and semantic segmentation [21, 27, 30].

However, the exploration of Vision Mamba’s potential within self-supervised learning remains relatively limited. Self-supervised pretraining methods such as Contrastive Learning (CL) [5, 11] and Masked Image Modeling (MIM) [1, 12, 29] have made substantial progress in computer vision, showcasing excellent performance through convolutional neural networks [18] and visual transformers [3, 7]. Nevertheless, when these methods are combined with Mamba [10, 16], they may not fully leverage the unique architectural features of Mamba. Notably, research on ARM [23] and MAP [15] suggests that autoregressive pretraining is better suited for Vision Mamba [16, 35].

The essence of autoregressive pretraining [4, 25, 32] lies in training models through the self-generative process of sequence data, allowing the models to gain a deep understanding of the intrinsic information within the data. In this process, models are trained by predicting the subsequent

\*Corresponding author.

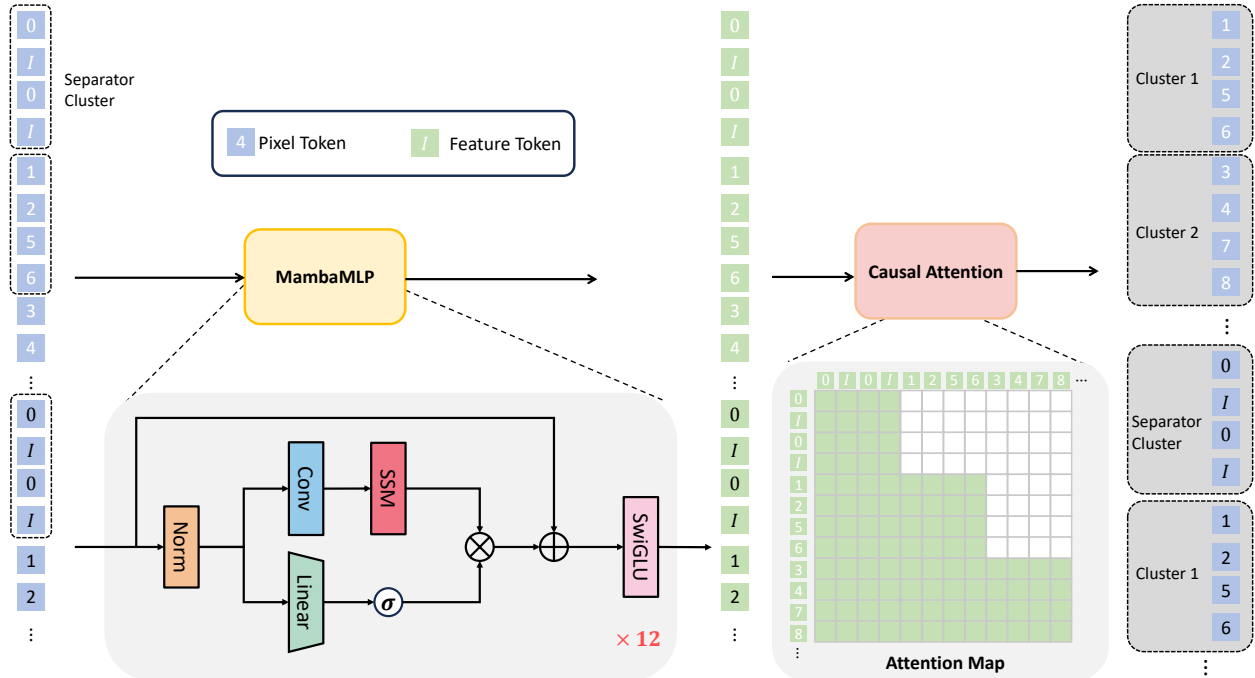


Figure 2. **Our STAR architecture.** During pretraining, we divide images into patches and group spatially adjacent patches into clusters. We then reorder the patches using a cluster-priority scanning method. Our STAR places a separator before the pixel patch sequence and merges multiple image sequences into a long sequence. This long sequence is fed into a MambaMLP with causal properties. The resulting feature tokens are input to a decoder with causal attention. The attention map of the decoder is bidirectional within clusters and unidirectional between clusters. This allows our STAR to treat clusters as the basic units for autoregressive prediction. The prediction target for the last cluster of one image is the separator cluster of the subsequent image.

element in a sequence. Since natural language is inherently 1D, it can naturally be modeled as sequential data, such as GPT-4 [20] and LLaMA2 [25]. However, images are 2D data, and modeling them for autoregressive pretraining tasks has posed a unique challenge. Numerous studies have embarked on this endeavor, leading to notable works such as iGPT [4], AIM [8], and ARM [23]. These methods target pixels, individual patches, and clusters of aggregated patches for reconstruction purposes, respectively. Although some success has been achieved, they are all short sequence modeling tasks for single images. Conversely, Mamba excels at handling long-sequence modeling tasks [33], creating a mismatch between pretraining task design and model capability. Current autoregressive pretraining methods fail to fully leverage the advantage of modern visual Mamba models in handling long sequence tasks.

In this paper, we propose a novel framework that adds a *Separator for AutoRegressive pretraining (STAR)* in Vision Mamba to form a long sequence task. The basic concept is illustrated in Fig. 1. Our innovation lies in introducing a unique, image-agnostic separator to each image, allowing multiple unrelated images to be modeled as a single long-sequence task. Specifically, each image is divided into non-overlapping patches, which are then grouped into

clusters of spatially adjacent patches. The size of the separator is the same as the cluster for each image. The diagonal patches of the separator are filled with vectors of ones, while the rest are filled with zero vectors. Then, we model multiple images with separators as a single long sequence following a row-major order, as depicted in Fig. 2. This long sequence comprises alternating segments of separators and pixel clusters. Finally, this long-sequence is fed into a causal encoder alongside a lightweight decoder, which sequentially predicts each cluster. Notably, the encoder is a unidirectional scanning Vision Mamba, while the decoder is a transformer with causal attention [31]. As shown in 2, the attention map is bidirectional within clusters and unidirectional between clusters. Compared to previous methods, our approach transcends the limitations of modeling single images, thereby expanding the possibilities of autoregressive pretraining. The primary advantage of our method is its ability to fully leverage Vision Mamba’s proficiency in handling long-sequence tasks through a long-sequence input. In our work, we explore variations in the types, values, positions, and numbers of separators. Unlike prior research on Vision Mamba [21, 35], we modify the position of the class token to enhance the advantages of long-sequence autoregressive pretraining. Our STAR positions the class to-

ken at the end of each image instead of in the middle. After 1600 epochs of autoregressive pretraining, our STAR-Base model achieves an accuracy of 83.5% on ImageNet-1k following end-to-end fine-tuning.

Our main contributions are summarized as follows:

- We propose a novel framework by introducing a separator within Vision Mamba that enables the modeling of multiple unrelated images as a single long-sequence task. This approach overcomes the limitations of traditional single-image modeling and fully leverages Vision Mamba’s advantages in handling long-sequence tasks.
- We modify the conventional setup of Vision Mamba by placing the class token at the end of each image, thereby enhancing the model’s performance in long-sequence tasks and achieving more efficient sequence modeling.
- Through end-to-end fine-tuning, our proposed method enables the STAR-Base model to achieve an accuracy of 82.9% on the ImageNet-1k dataset, demonstrating the effectiveness and practicality of the approach in image classification tasks.

## 2. Related Work

**Vision Mamba.** Building on Mamba’s success in the NLP domain and its demonstrated potential to replace transformers, there has been a surge in the development of visual models based on Mamba [10, 19]. Vision Mamba pioneers this effort through the introduction of the Vim block [35], which leverages pure Mamba layers. Each Vim block employs forward and backward scanning to construct bidirectional representations, thereby adapting the 1D-based Mamba architecture for 2D image processing. Subsequently, Vmamba [16] introduces Visual State Space (VSS) blocks, which integrate Mamba with 2D convolution layers. Adopting a pyramid structure akin to the Swin Transformer [17], each VSS block initially models 2D local information via two-dimensional depth convolutions, serving as token mixers. This is followed by the processing of 2D global information in both horizontal and vertical directions through a cross-scanning module. In the pursuit of advancing Mamba’s self-supervised pretraining capabilities, the ARM model [23] incorporates a streamlined MambaMLP block. This module uses Mamba for token mixing and a multi-layer perceptron (MLP) for channel mixing. ARM successfully scales Vision Mamba models through autoregressive pretraining. To concentrate more effectively on autoregressive pretraining, we select the MambaMLP model as the focal point of our study.

**Autoregressive Pretraining in Vision.** Autoregressive pretraining [9, 13, 32] is an advanced machine learning technique widely used in model training for fields such as natural language processing and computer vision [4, 8, 15,

23]. The core idea is to train the model through a self-generative process of sequential data, allowing the model to gain a deep understanding of the underlying structure and patterns within the data. In this process, the model learns the distributional characteristics of the data by predicting the next token in the sequence.

In the field of computer vision, autoregressive pretraining experiences several phases of development. iGPT [4] is among the first to explore this approach in CV by treating each pixel in an image as an independent element. By serializing image pixels, iGPT facilitates autoregressive training to generate realistic new images and achieve unsupervised representation learning. Subsequently, AIM [8] investigates a patch-based autoregressive training method. Through enlarging the pretraining datasets and expanding model parameters, AIM [8] demonstrates that autoregression can also achieve success in CV. Nevertheless, these methods are predominantly based on transformers. ARM [23] pioneers the application of autoregressive pretraining on the Vision Mamba model. It segments images into non-overlapping patches and then aggregates adjacent patches into clusters. By applying autoregressive pretraining to these clusters, ARM empirically validates the scalability of the Vision Mamba model.

Regardless of whether the approach is based on pixels, patches, or clusters, all these autoregressive pretraining techniques are executed on individual images. ARM [23] does not utilize the Mamba model’s potential for handling long-sequence tasks. Therefore, we are the first to model autoregressive pretraining as a long-sequence task, aiming to explore the substantial potential of Vision Mamba.

**Other Self-supervised learning** approaches include contrastive learning and masked image modeling, *etc.* These self-supervised models [5, 34] are renowned for their ability to learn powerful transferable features from unlabeled data. Contrastive learning [2, 5, 6] has been particularly popular, achieving this goal by modeling the similarity and dissimilarity (or simply similarity) between two or more views of an image. Masked image models [1, 12, 28], on the other hand, attempt to learn more robust features by recovering the complete image from a corrupted version. However, in ARM [23], experiments have shown that these self-supervised learning methods are not well-suited for the Mamba model. Our work seeks to explore self-supervised pretraining within Mamba through autoregressive pretraining, pursuing a conceptually distinct direction.

## 3. Method

### 3.1. Mamba Preliminaries

Mamba [10, 35] is an effective state space model (SSM) with linear computation complexity. SSMs can be regarded

as linear time-invariant (LTI) systems that maps the input  $x(t) \in \mathbb{R}$  to output  $y(t) \in \mathbb{R}$  through a hidden state  $h(t) \in \mathbb{R}^{d \times 1}$ . Concretely, continuous-time SSMs can be formulated as linear ordinary differential equations (ODEs) as follows,

$$\begin{aligned} h'(t) &= \mathbf{A}h(t) + \mathbf{B}x(t), \\ y(t) &= \mathbf{C}h(t), \end{aligned} \quad (1)$$

where  $\mathbf{A} \in \mathbb{R}^{d \times d}$  is the evolution parameter.  $\mathbf{B} \in \mathbb{R}^{d \times 1}$  and  $\mathbf{C} \in \mathbb{R}^{1 \times d}$  are the projection parameters.

To be applied to deep neural networks, SSM is first transformed into its discrete version through zero-order hold discretization. Specifically, the continuous parameters  $\mathbf{A}, \mathbf{B}$  are transformed to discrete parameters  $\bar{\mathbf{A}}, \bar{\mathbf{B}}$  using a timescale parameters  $\Delta \in \mathbb{R}$ :

$$\begin{aligned} \bar{\mathbf{A}} &= \exp(\Delta \mathbf{A}), \\ \bar{\mathbf{B}} &= (\Delta \mathbf{A})^{-1}(\exp(\Delta \mathbf{A}) - I) \cdot \Delta \mathbf{B}. \end{aligned} \quad (2)$$

After the discretization of  $\bar{\mathbf{A}}, \bar{\mathbf{B}}$ , the discretized version of Eq. (1) using a step size  $\Delta$  can be rewritten as:

$$\begin{aligned} h_t &= \bar{\mathbf{A}}h_{t-1} + \bar{\mathbf{B}}x_t, \\ y_t &= \mathbf{C}h_t. \end{aligned} \quad (3)$$

Then we can employ a matrix  $\bar{\mathbf{K}}$  for fast computation:

$$\begin{aligned} \bar{\mathbf{K}} &= (\mathbf{C}\bar{\mathbf{B}}, \mathbf{C}\bar{\mathbf{A}}\bar{\mathbf{B}}, \dots, \mathbf{C}\bar{\mathbf{A}}^k\bar{\mathbf{B}}), \\ \mathbf{y} &= \mathbf{x} * \bar{\mathbf{K}}, \end{aligned} \quad (4)$$

where  $k \in [0, L]$  and  $L$  is the length of the input sequence  $\mathbf{x}$ . We also have  $\mathbf{y} = \{y_1, \dots, y_L\}$ ,  $\mathbf{x} = \{x_1, \dots, x_L\}$ , while  $\bar{\mathbf{K}} \in \mathbb{R}^L$  is a structured convolutional kernel. Due to the inherent causality of SSMs, they are particularly well-suited for autoregressive pretraining.

In this paper, we use the MambaMLP [23] as the backbone, as shown in Fig. 2. MambaMLP block uses Mamba as the token mixer and multi-layer perceptron (MLP) as the channel mixer. In the autoregressive pretraining, the MambaMLP block contains the Mamba layer with only 1 scan to match the uni-directional modeling manner. However, the block is adapted to contain the Mamba layer with 4 scans, thus enabling bi-directional modeling of global information analogous to that in Vmamba [16].

### 3.2. Autoregressive pretraining

We begin by introducing the vanilla version of autoregressive pretraining. Next, we discuss the current autoregressive pretraining method in the field of computer vision. Finally, we present our improved version that addresses the existing challenges of autoregressive pretraining in computer vision.

#### 3.2.1 Next Token Prediction

The next token prediction is the most classic task of Autoregressive (AR) pretraining and has become one of the key factors contributing to the success of large language models (LLMs) [20, 25]. Its core principle involves predicting the next token sequentially, based on the preceding input tokens. For a given input from a corpus  $\mathcal{U} = \{u_1, \dots, u_n\}$ , the probability of the corpus can be factorized as a product of token conditional probabilities:

$$P(u) = \prod_{k=1}^n P(u_k | u_{<k}, f_\theta), \quad (5)$$

where  $u_{<k}$  denotes the set of the first  $k-1$  tokens and is the context used to predict the  $k^{\text{th}}$  token.  $f_\theta$  is a neural network with parameters  $\theta$ .

Autoregressive pretraining computes the likelihood of each token  $u_k$  based on the context of all preceding tokens from  $u_1$  to  $u_{k-1}$  and minimizes the negative log-likelihood:

$$\mathcal{L} = -\log P(u).$$

#### 3.2.2 Autoregressive pretraining in Vision

In the field of computer vision, input images are inherently 2D structures and lack a natural sequential order. To adapt autoregressive pretraining for image data effectively, it is necessary to artificially construct a sequence that imposes a specific order. Several prior works, including iGPT, AiM, and ARM, have explored this approach, each with varying levels of sequence granularity. In this paper, we adopt the framework proposed by ARM to guide our methodology.

Given a natural image  $X$  from an unlabeled dataset  $\mathcal{D}_u$ , we first reshape it into  $n$  patches, denoted as  $X = \{P_1, \dots, P_n\} \in \mathbb{R}^{n \times s}$  where  $s$  denotes the path size and  $P_i \in \mathbb{R}^s$  is the  $i^{\text{th}}$  patch. To encapsulate the 2D spatial information at the token level, we group spatially adjacent image patches into larger clusters to serve as the prediction unit, as illustrated in Fig. 1. For the clustered input  $X = \{c_1, \dots, c_L\}$ , the loss function of autoregressive pretraining is denoted as:

$$\mathcal{L} = \sum_{i=1}^{L-1} |f(c_{\leq i}, c_{i+1})|^2, \quad (6)$$

where each  $c_i \in \mathbb{R}^{H_c \times W_c}$  is a cluster formed by grouping  $\frac{H_c}{16} \times \frac{W_c}{16}$  patches and  $c_{\leq i}$  denotes the set of the first  $i$  clusters.  $L$  is the number of the clusters. An encoder  $f$  is a MambaMLP-based network with 1 scan.

### 3.3. Separator for AR

Firstly, since autoregressive pretraining is conducted using clusters as the basic unit, this means that at least  $\frac{1}{L}$  (default

$L = 9$ ) of the image information is not utilized, as the information from the first cluster is not used for prediction. Secondly, during the autoregressive pretraining phase, each image is set to a fixed size, which means that the length of tokens received by the encoder for a single image is relatively short. This prevents fully leveraging the Mamba series model’s strength in handling long-sequence tasks. To address these challenges, we introduce separators, which offer a unified solution to both issues.

For each clustered input  $X = \{c_1, \dots, c_L\}$ , we add a *separator cluster*  $c_{sp}$ . Specifically,  $c_{sp}$  is constructed as a cluster of *alternating 0 and 1 tokens*, matching the length of  $c_i$  ( $i \in [1, L]$ ). This separator cluster  $c_{sp}$  is placed at the beginning of all other clusters to signify the start of an image. Thus, each image is represented as  $X = \{c_0, c_1, \dots, c_L\}$  where  $c_0 := c_{sp}$ .

With the addition of  $c_{sp}$ , we can represent multiple images within the same sequence, using  $c_{sp}$  as a separator. This approach allows us to extend the length of the input tokens for the encoder, effectively constructing a long-sequence version of autoregressive pretraining. The input of the encoder  $f$  denotes as  $I = \{X_1, \dots, X_N\} = \{c_0^1, c_1^1, \dots, c_L^1, c_0^2, \dots, c_L^N\}$ . Therefore, the loss function of our autoregressive pretraining with the separator  $c_{sp}$  is denoted as:

$$\mathcal{L}_{STAR} = \sum_{i=0}^{L*N} |f(c_{\leq i}, c_{i+1})|^2, \quad (7)$$

where  $L$  denotes the number of clusters and  $N$  represents the number of images within the input sequence. Let  $c_{L*N+1} := c_{sp}$ . The pixel values  $f(c_{\leq i})$  are all normalized, using the same method as in MAE [12].

Our method is illustrated in Fig. 2. Our method initiates the step-by-step reconstruction from the first cluster that holds pixel significance. By doing so, it ensures the full utilization of all information available in each image. Furthermore, by incorporating multiple images within a single input sequence, the method not only enables the model to capture cross-image dependencies but also enhances the robustness and diversity of the training process. This approach allows the model to learn more comprehensive features and patterns across different images, ultimately improving its performance on downstream tasks.

## 4. Experiment

### 4.1. Experiment Settings

**Pretraining** We conduct autoregressive pretraining on the ImageNet-1k training set, which consists of approximately 1.28 million images. Similar to the approach used in MAE, we apply two data augmentation techniques, namely random cropping and horizontal flipping. Throughout all experiments, we utilize MambaMLP as the backbone. Dur-

ing the autoregressive pretraining phase, the MambaMLP blocks are configured to include only a single-scan Mamba layer, aligning with the unidirectional modeling approach. In autoregressive pretraining, we employ an AdamW optimizer with a *cosine* learning rate scheduler and train for 200 epochs. The training parameters are: the batch size as 2048, the learning rate as  $\text{lr} = 1.5\text{e-}4 \times \frac{\text{batchsize}}{256}$ , weight decay as 0.05,  $\beta_1 = 0.9$ ,  $\beta_2 = 0.95$ , warm-up for 40 epochs.

The default options for the components of STAR are: a separator cluster with  $4 \times 4$  patches, an input sequence with 8 images. Our decoder is a lightweight, 4-layer network based on cross-attention mechanisms, where each layer has a width of 512.

**Finetuning** In finetuning, we also employ an AdamW optimizer, 100-epoch training, and a cosine learning rate scheduler with 5-epoch warm-up. The finetuning hyperparameters are: the batch size as 1024, the learning rate as  $\text{lr} = 5\text{e-}4 \times \frac{\text{batchsize}}{256}$ , a weight decay of 0.05, a stochastic depth ratio of 0.1, and a layer-wise learning rate decay of 0.65. We follow the same data augmentation used in MAE, including RandAug, Mixup, Cutmix, and label smoothing. Additionally, we employ the exponential moving average (EMA) for stronger performance. To enhance the adaptability of Mamba for 2D vision data, we follow the Vmamba strategy during downstream task fine-tuning. Specifically, we employed four scanning paths in MambaMLP to comprehensively traverse the data.

### 4.2. Main Properties

As this paper represents the first investigation of separators within the field of computer vision, there is extensive work required to explore their characteristics. Given our resource constraints, we focus our exploration of separators on several key aspects, including their type, value, position, and number.

**Separator type.** We initially investigate the impact of various types of separators on the effectiveness of representation learning. Tab. 1 summarizes the finetuning accuracy and EMA accuracy achieved with different types of separators. In the experiments evaluating different types of separators, we concatenate 4 images into a single sequence. We consider three types of separators: no separator, token-based separators, and cluster-based separators.

Firstly, we examine the impact of merely extending the input sequence length without any additional modifications. Concatenating sequences of four images into a single sequence without separators leads to a noticeable drop in performance, as evidenced by a decline in EMA (Exponential Moving Average) accuracy from 82.15% to 78.63%. This suggests that direct interaction between different images is ineffective. Subsequently, we introduce a separator

Type	Backbone	Epochs	FT (%)	EMA (%)
Baseline	MambaMLP-B	200	81.81	82.15
None	MambaMLP-B	200	78.64	78.63
Token	MambaMLP-B	200	79.41	79.37
Cluster	MambaMLP-B	200	<b>82.15</b>	<b>82.40</b>

Table 1. **Finetuning accuracy (%) and EMA accuracy (%) of pretrained models by different types of separators on ImageNet-1K.** The best for each column is **bolded**.

configured as a zero-vector token. After end-to-end finetuning, the EMA accuracy increases to 79.37%, marking a 0.74% improvement over the configuration without separators. This indicates that maintaining independence between images through separators provides certain benefits to long-sequence autoregressive modeling. However, the performance of the token-based separator still falls short compared to autoregressive training on a single image. We suggest that this discrepancy arises due to a mismatch between the separator and the fundamental unit of autoregressive prediction: the separator is a single token, whereas the basic prediction unit comprises a cluster of 4x4 tokens.

Finally, we set the separator as a cluster. A zero-vector token is expanded into a 4x4 token cluster, with shared positional encoding across the tokens. We place the cluster-based separator at the start of each image, as illustrated in Fig. 2, and reconstruct each cluster sequentially. The cluster-based separator achieves an accuracy of 82.15% and an EMA accuracy of 82.40%, representing improvements of 0.34% and 0.25% over autoregressive pretraining on a single image, respectively. This demonstrates that a suitable separator can significantly enhance autoregressive pretraining performance, highlighting the critical role of separators in long-sequence autoregressive pretraining.

**Separator value.** This study introduces the concept of separators in the field of computer vision for the first time. As a novel concept, the specific form of separators has not yet been established, with the most critical aspect being their exact values. It is essential to ensure that separators are distinct. Therefore, separators should neither conflict with existing pixel information nor obscurely separate different images. In our exploration, we considered four potential values: a cluster of all-zero vectors, a cluster of all-one vectors, a cluster utilizing  $nn.embedding(0)$ , and a cluster with alternating zero and one vectors. Fig. 3 illustrates these different types of separators. For ease of reference in subsequent discussions, we refer to them as the *Zeros* separator, *Ones* separator, *Embeddings* separator, and *Identity* separator, respectively.

We concatenate 8 images into a single long sequence. All these separators are placed at the beginning of each image and bypass the patch embedding layer. The experimental results are shown in Tab. 2, where it is evident that all

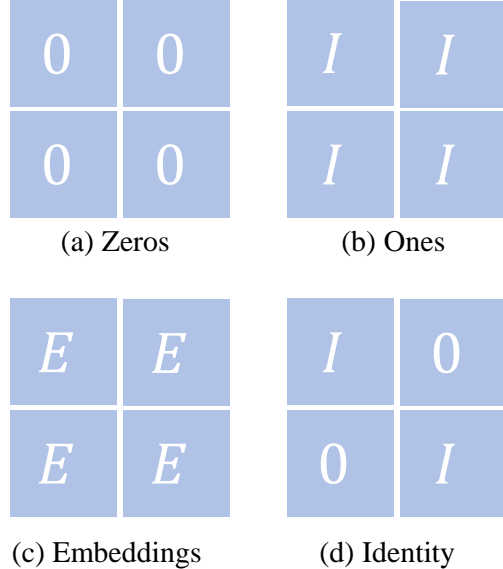


Figure 3. **Different values of Separator.** **Zeros:** all tokens in the cluster are zero vectors. **Ones:** all tokens in the cluster are one vectors. **Embeddings:** all tokens in the clusters are  $nn.embedding(0)$ . **Identity:** tokens on the diagonal of the cluster are one vectors, while other tokens are zero vectors.

Value	Backbone	Epochs	FT (%)	EMA (%)
Baseline	MambaMLP-B	200	81.81	82.15
Zeros	MambaMLP-B	200	81.77	<b>82.35</b>
Ones	MambaMLP-B	200	81.83	82.26
Embeddings	MambaMLP-B	200	<b>82.05</b>	82.27
Identity	MambaMLP-B	200	<u>82.03</u>	<u>82.32</u>
Zeros	MambaMLP-B	300	81.79	82.54
Identity	MambaMLP-B	300	<b>82.08</b>	<b>82.58</b>

Table 2. **Finetuning accuracy (%) and EMA accuracy (%) of pretrained models by different values of separators on ImageNet-1K.** The best for each column is **bolded**. The second for each column is underline.

four types of separators significantly enhance autoregressive pretraining performance. Specifically, the *Zeros* separator achieves the highest EMA accuracy at 82.35%, while the embeddings separator achieves the highest basic accuracy at 82.05%. The identity separator ranks second in both basic accuracy and the EMA accuracy.

To further validate the value of the separator, we extend the number of training epochs. When autoregressive pretraining is conducted for 300 epochs, the *Identity* separator exhibited superior performance, achieving basic and EMA accuracies of 82.08% and 82.58%, respectively. Considering both the basic accuracy and the EMA accuracy, we select the *Identity* separator as our separator. However, for studies on separators, we set the default to the simplest *Zeros* separator.

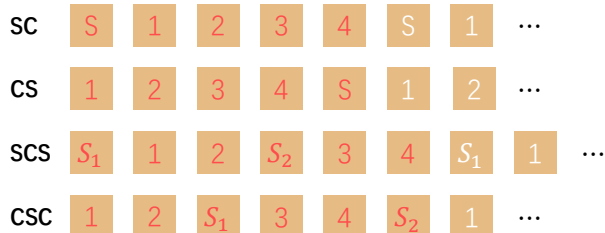


Figure 4. **Different positions of Separator.** **SC**: separator is placed before the cluster. **CS**: separator is placed after the cluster. **SCS**: separator and cluster appear alternately, with the initial separator placed before the cluster. **CSC**: separator and cluster appear alternately, with the initial separator placed after the cluster.

Position	Epochs	Time (h)	FT (%)	EMA (%)
SC	200	24.6	<u>81.77</u>	<b>82.35</b>
CS	200	24.6	77.93	77.94
SCS	200	31.4	<b>81.98</b>	<u>82.33</u>
CSC	200	31.4	78.69	78.64

Table 3. **Finetuning accuracy (%) and EMA accuracy (%) of pretrained models by different positions of separators on ImageNet-1K.** The best for each column is **bolded**. The second for each column is underline

**Separator position.** We conduct an in-depth investigation into the insertion positions of the separator. Two primary configurations are considered: placing the separator before the other clusters within an image, termed as **SC**, and placing it after the clusters, referred to as **CS**. Additionally, we explore denser separator layouts: after dividing an image into  $n^2$  clusters, a separator is inserted every  $n$  clusters. This dense configuration is further divided into two variations: inserting the separator before the cluster, denoted as **SCS**, and after the cluster, denoted as **CSC**. Fig. 4 illustrates these different layout strategies in detail.

Tab. 3 presents the fine-tuning accuracy (FT) and exponential moving average accuracy (EMA) on ImageNet-1K for different separator positions in the pre-trained models. We compare both accuracy and training time. The SC configuration performs best, achieving the highest EMA accuracy (82.35%) and second-best FT accuracy (81.77%) after 24.6 hours of training. The SCS configuration attains the highest FT accuracy (81.98%) and the second-highest EMA accuracy, but requires an extended training time of 31.4 hours. The CS and CSC configurations perform poorly, with accuracies falling below 79%. This indicates that the position of the separator significantly impacts model performance, with the SC configuration striking the optimal balance between accuracy and training efficiency. The superior performance observed when the separator is positioned before clusters may be due to ensuring the integrity of each image’s reconstruction. When the separator is placed after

Num	Backbone	Epochs	FT (%)	EMA (%)
1	MambaMLP-B	200	81.94	82.20
2	MambaMLP-B	200	81.92	82.24
4	MambaMLP-B	200	<b>82.15</b>	<b>82.40</b>
8	MambaMLP-B	200	81.77	82.35
16	MambaMLP-B	200	81.55	81.97

Table 4. **Finetuning accuracy (%) and EMA accuracy (%) of pretrained models by different numbers of separators on ImageNet-1K.** The best for each column is **bolded**.

Model	Epochs	FT (%)	EMA (%)
STAR-B	200	81.77	82.35
STAR-B	300	81.79	82.54
STAR-B*	200	81.89	82.61
STAR-B*	300	<b>82.18</b>	<b>82.86</b>

Table 5. **Finetuning accuracy (%) and EMA accuracy (%) of pretrained models by different class token on ImageNet-1K.** The best for each column is **bolded**. \* indicates that the tail class token is used.

clusters, the first cluster of the sequence’s initial image is excluded from prediction.

**Separator number.** When extending the sequence length for autoregressive pretraining, it is crucial to explore the upper limit of the input sequence length. This exploration helps us understand the model’s capacity and optimize its performance. We conduct a series of experiments varying the number of images in a sequence, ranging from 1 to 16. Each image in our setup comprises 144 tokens for the image content plus 16 separator tokens, totaling 160 tokens per image.

Consequently, the input length for each model in our experiments spans from 160 tokens (for a single image) to 2,560 tokens (for 16 images). Tab. 4 presents the comprehensive results of these experiments, showing how model performance varies with input length. Notably, when the number of images is set to 4, resulting in a total of 640 tokens, both the basic accuracy and EMA accuracy peak at 82.15% and 82.4%, respectively. This finding is particularly significant as it suggests that MambaMLP exhibits optimal feature extraction capabilities when processing input sequences of around 640 tokens. However, longer sequences do not necessarily yield better performance. When the model processes sequences as long as 2560 tokens, a decline in performance is observed, suggesting that the length bottleneck of MambaMLP-B might have been approached.

**Tail class token.** To better adapt the long-sequence autoregressive pretraining model for classification tasks, we adjust the position of the class token. The existing Vision

Mamba model, following the Vim setup, typically places the class token in the middle of the sequence. However, a long-sequence autoregressive pretraining model gains a more comprehensive understanding of the image through the autoregressive task and captures relationships across the long sequence more effectively. Therefore, we reposition the class token at the end of the visual sequence. We perform re-tuning for our STAR model based on this configuration. The results are shown in Tab. 5. After 300 epochs of autoregressive pretraining, the STAR-B model with the class token at the end achieves an EMA accuracy of 82.86%, an improvement of 0.3% over the original configuration. This indicates that after long-sequence autoregressive pretraining, our STAR can develop a clear understanding of a complete image sequence.

### 4.3. Comparisons with Previous Results

**Comparisons with self-supervised methods.** We use MambaMLP as the backbone to compare several self-supervised methods, including contrastive learning, MAE, and ARM. All methods are trained for 300 epochs. We employ an input resolution of  $224 \times 224$  to align with previous approaches. Detailed experimental results are presented in Tab. 6. For a more comprehensive evaluation, we also compare the training times required by different methods. Through fine-tuning, our method achieves a peak accuracy of 82.9%, outperforming the previous best method by 0.4%. Moreover, our method shows exceptional training efficiency—6.6 times and 1.4 times more efficient than contrastive learning and MAE, respectively. Our results are based on the vanilla Vision Mamba, and we believe more advanced networks could yield even better performance. Compared to ARM, our STAR is not only more accurate but also simpler. We design a long-sequence pretraining task for Mamba, with an input length eight times that of ARM. Notably, our STAR does not require any special modifications to image dimensions.

Furthermore, we specifically include in Tab. 6 the results achieved by ViT-B under various self-supervised pretraining methods. Despite the fact that our STAR exhibits significantly lower computational complexity compared to ViT-B, it still demonstrates strong competitiveness. MAE [12] achieves an accuracy of 83.6% on ViT-B, while our STAR-B also reached an accuracy of 83.5%, nearly on par with it.

**Comparisons with other lightweight models.** In recent years, a surge of high-performance lightweight models has emerged. We select representative models from convolutional neural networks, Vision Transformers, and Vision Mamba for comparison. These models all boast high throughput and impressive performance. Tab. 7 presents the specific experimental results. Our STAR model achieves very competitive performance among lightweight models,

Method	Backbone	Epochs	Time (h)	EMA (%)
MoCov3 [6]	ViT-B	300	-	83.0
MoCov3 [6]	ViT-B	600	-	83.2
MAE [12]	ViT-B	300	-	82.9
MAE [12]	ViT-B	1600	-	<b>83.6</b>
AR <sup>†</sup>	ViT-B	300	-	82.5
Supervised	MambaMLP-B	300	110	81.2
Contrastive	MambaMLP-B	300	330	81.4
MAE	MambaMLP-B	300	70	81.6
ARM	MambaMLP-B	300	34	82.5
ARM	MambaMLP-B	1600	182	83.2
STAR*	MambaMLP-B	300	50	82.9
STAR*	MambaMLP-B	1600	267	<u>83.5</u>

Table 6. **Finetuning accuracy (%) and EMA accuracy (%) of pretrained models by different numbers of separators on ImageNet-1K.** The best for each column is **bolded**. The second for each column is underline.<sup>†</sup> means the result is borrowed from [15]. \* indicates that the tail class token is used.

Model	Token Mixer	Param. (M)	Throughputs (imgs/s)	Top-1 Top-1 (%)
RegNetY-16G [22]	2D Conv.	84	870	82.9
DeiT-B [24]	Attention	21	1073	81.2
Vim-B [35]	Mamba	98	890	81.2
MambaMLP-B [23]	Mamba	85	1301	81.2
VMamba-B	Mamba+2D Conv.	89	315	<b>83.9</b>
STAR-B*	Mamba	85	1301	82.9
STAR-B* <sup>††</sup>	Mamba	85	1301	<u>83.5</u>

Table 7. **Finetuning accuracy (%) and EMA accuracy (%) of pretrained models by different numbers of separators on ImageNet-1K.** The best for each column is **bolded**. The second for each column is underline. \* indicates that the tail class token is used. <sup>††</sup> indicates that the pretraining epochs are 1600.

matching RegNetY-16G [22] with an accuracy of 82.9%. Unlike supervised training models that have reached performance saturation, STAR still has room for improvement. We anticipate even better performance by extending the self-regressive pretraining epochs. After 1600 epochs of autoregressive pretraining, our STAR-B achieves an accuracy of 83.5% on Imagenet-1k, which is comparable to that of VMamba [16].

## 5. Discussion and Conclusion

In this paper, we propose a novel long-sequence autoregressive pretraining framework called STAR. To enhance the autoregressive pretraining performance on Vision Mamba, we add a separator for each image. The article conducts an in-depth study of the separator from four aspects: type, value, position, and quantity. Furthermore, we modify the cls token of STAR to fully utilize Vision Mamba’s capability in handling long sequence tasks. The uniqueness of STAR lies in its potential for improvement—by extending the autoregressive pretraining, it is expected to achieve even better performance. Overall, STAR provides a highly

promising new direction for the field of computer vision, especially in the design and training of lightweight models.

## References

- [1] Hangbo Bao, Li Dong, Songhao Piao, and Furu Wei. Beit: BERT pre-training of image transformers. In *ICLR 2022*, 2022. 1, 3
- [2] Mathilde Caron, Hugo Touvron, Ishan Misra, Hervé Jégou, Julien Mairal, Piotr Bojanowski, and Armand Joulin. Emerging properties in self-supervised vision transformers. In *ICCV 2021*, pages 9630–9640, 2021. 3
- [3] Chun-Fu (Richard) Chen, Quanfu Fan, and Rameswar Panda. Crossvit: Cross-attention multi-scale vision transformer for image classification. In *ICCV 2021*, pages 347–356, 2021. 1
- [4] Mark Chen, Alec Radford, Rewon Child, Jeffrey Wu, Heewoo Jun, David Luan, and Ilya Sutskever. Generative pre-training from pixels. In *ICML 2020*, pages 1691–1703, 2020. 1, 2, 3
- [5] Ting Chen, Simon Kornblith, Mohammad Norouzi, and Geoffrey E. Hinton. A simple framework for contrastive learning of visual representations. In *ICML 2020*, pages 1597–1607, 2020. 1, 3
- [6] Xinlei Chen, Saining Xie, and Kaiming He. An empirical study of training self-supervised vision transformers. In *ICCV 2021*, pages 9620–9629, 2021. 3, 8
- [7] Alexey Dosovitskiy, Lucas Beyer, Alexander Kolesnikov, Dirk Weissenborn, Xiaohua Zhai, Thomas Unterthiner, Mostafa Dehghani, Matthias Minderer, Georg Heigold, Sylvain Gelly, Jakob Uszkoreit, and Neil Houlsby. An image is worth 16x16 words: Transformers for image recognition at scale. In *ICLR 2021*, 2021. 1
- [8] Alaaeldin El-Nouby, Michal Klein, Shuangfei Zhai, Miguel Ángel Bautista, Vaishaal Shankar, Alexander T. Shev, Joshua M. Susskind, and Armand Joulin. Scalable pre-training of large autoregressive image models. In *ICML 2024*, 2024. 2, 3
- [9] Alaaeldin El-Nouby, Michal Klein, Shuangfei Zhai, Miguel Ángel Bautista, Vaishaal Shankar, Alexander T. Shev, Joshua M. Susskind, and Armand Joulin. Scalable pre-training of large autoregressive image models. In *ICML 2024*, 2024. 3
- [10] Albert Gu and Tri Dao. Mamba: Linear-time sequence modeling with selective state spaces. *CoRR*, abs/2312.00752, 2023. 1, 3
- [11] Kaiming He, Haoqi Fan, Yuxin Wu, Saining Xie, and Ross B. Girshick. Momentum contrast for unsupervised visual representation learning. In *CVPR 2020*, pages 9726–9735, 2020. 1
- [12] Kaiming He, Xinlei Chen, Saining Xie, Yanghao Li, Piotr Dollár, and Ross B. Girshick. Masked autoencoders are scalable vision learners. In *CVPR 2022*, pages 15979–15988, 2022. 1, 3, 5, 8
- [13] Tianyu Hua, Yonglong Tian, Sucheng Ren, Michalis Raptis, Hang Zhao, and Leonid Sigal. Self-supervision through random segments with autoregressive coding (randsac). In *ICLR 2023*, 2023. 3
- [14] Rudolph Emil Kalman. A new approach to linear filtering and prediction problems. 1960. 1
- [15] Yunze Liu and Li Yi. MAP: unleashing hybrid mamba-transformer vision backbone’s potential with masked autoregressive pretraining. *CoRR*, abs/2410.00871, 2024. 1, 3, 8
- [16] Yue Liu, Yunjie Tian, Yuzhong Zhao, Hongtian Yu, Lingxi Xie, Yaowei Wang, Qixiang Ye, and Yunfan Liu. Vmamba: Visual state space model. *CoRR*, abs/2401.10166, 2024. 1, 3, 4, 8
- [17] Ze Liu, Yutong Lin, Yue Cao, Han Hu, Yixuan Wei, Zheng Zhang, Stephen Lin, and Baining Guo. Swin transformer: Hierarchical vision transformer using shifted windows. In *ICCV 2021*, pages 9992–10002, 2021. 3
- [18] Zhuang Liu, Hanzi Mao, Chao-Yuan Wu, Christoph Feichtenhofer, Trevor Darrell, and Saining Xie. A convnet for the 2020s. In *CVPR 2022*, pages 11966–11976, 2022. 1
- [19] Harsh Mehta, Ankit Gupta, Ashok Cutkosky, and Behnam Neyshabur. Long range language modeling via gated state spaces. In *ICLR 2023*, 2023. 3
- [20] OpenAI. GPT-4 technical report. *CoRR*, abs/2303.08774, 2023. 2, 4
- [21] Xiaohuan Pei, Tao Huang, and Chang Xu. Efficientvmamba: Atrous selective scan for light weight visual mamba. *CoRR*, abs/2403.09977, 2024. 1, 2
- [22] Ilija Radosavovic, Raj Prateek Kosaraju, Ross B. Girshick, Kaiming He, and Piotr Dollár. Designing network design spaces. In *CVPR 2020*, pages 10425–10433, 2020. 8
- [23] Sucheng Ren, Xianhang Li, Haoqin Tu, Feng Wang, Fangxun Shu, Lei Zhang, Jieru Mei, Linjie Yang, Peng Wang, Heng Wang, Alan L. Yuille, and Cihang Xie. Autoregressive pretraining with mamba in vision. *CoRR*, abs/2406.07537, 2024. 1, 2, 3, 4, 8
- [24] Hugo Touvron, Matthieu Cord, Matthijs Douze, Francisco Massa, Alexandre Sablayrolles, and Hervé Jégou. Training data-efficient image transformers & distillation through attention. In *ICML 2021*, pages 10347–10357, 2021. 8
- [25] Hugo Touvron, Louis Martin, Kevin Stone, Peter Albert, Amjad Almahairi, Yasmine Babaei, Nikolay Bashlykov, Soumya Batra, Prajjwal Bhargava, Shrutvi Bhosale, Dan Bikel, Lukas Blecher, Cristian Canton-Ferrer, Moya Chen, Guillem Cucurull, David Esiobu, Jude Fernandes, Jeremy Fu, Wenyin Fu, Brian Fuller, Cynthia Gao, Vedanuj Goswami, Naman Goyal, Anthony Hartshorn, Saghar Hosseini, Rui Hou, Hakan Inan, Marcin Kardas, Viktor Kerkez, Madian Khabsa, Isabel Kloumann, Artem Korenev, Punit Singh Koura, Marie-Anne Lachaux, Thibaut Lavril, Jenya Lee, Diana Liskovich, Yinghai Lu, Yuning Mao, Xavier Martinet, Todor Mihaylov, Pushkar Mishra, Igor Molybog, Yixin Nie, Andrew Poulton, Jeremy Reizenstein, Rashi Rungta, Kalyan Saladi, Alan Schelten, Ruan Silva, Eric Michael Smith, Ranjan Subramanian, Xiaoqing Ellen Tan, Binh Tang, Ross Taylor, Adina Williams, Jian Xiang Kuan, Puxin Xu, Zheng Yan, Iliyan Zarov, Yuchen Zhang, Angela Fan, Melanie Kambadur, Sharan Narang, Aurélien Rodriguez, Robert Stojnic, Sergey Edunov,

- and Thomas Scialom. Llama 2: Open foundation and fine-tuned chat models. *CoRR*, abs/2307.09288, 2023. 1, 2, 4
- [26] Feng Wang, Jiahao Wang, Sucheng Ren, Guoyizhe Wei, Jieru Mei, Wei Shao, Yuyin Zhou, Alan L. Yuille, and Cihang Xie. Mamba-r: Vision mamba ALSO needs registers. *CoRR*, abs/2405.14858, 2024. 1
- [27] Ziyang Wang, Jian-Qing Zheng, Yichi Zhang, Ge Cui, and Lei Li. Mamba-unet: Unet-like pure visual mamba for medical image segmentation. *CoRR*, abs/2402.05079, 2024. 1
- [28] Chen Wei, Haoqi Fan, Saining Xie, Chao-Yuan Wu, Alan L. Yuille, and Christoph Feichtenhofer. Masked feature prediction for self-supervised visual pre-training. In *CVPR 2022*, pages 14648–14658, 2022. 3
- [29] Zhenda Xie, Zheng Zhang, Yue Cao, Yutong Lin, Jianmin Bao, Zhuliang Yao, Qi Dai, and Han Hu. Simmim: a simple framework for masked image modeling. In *CVPR 2022*, pages = 9643–9653, year = 2022,. 1
- [30] Zhaohu Xing, Tian Ye, Yijun Yang, Guang Liu, and Lei Zhu. Segmamba: Long-range sequential modeling mamba for 3d medical image segmentation. In *MICCAI 2024*, pages 578–588, 2024. 1
- [31] Xu Yang, Hanwang Zhang, Guojun Qi, and Jianfei Cai. Causal attention for vision-language tasks. In *CVPR 2021*, pages 9847–9857, 2021. 2
- [32] Zhilin Yang, Zihang Dai, Yiming Yang, Jaime G. Carbonell, Ruslan Salakhutdinov, and Quoc V. Le. Xlnet: Generalized autoregressive pretraining for language understanding. In *NeurIPS 2019*,, pages 5754–5764, 2019. 1, 3
- [33] Weihao Yu and Xinchao Wang. Mambaout: Do we really need mamba for vision? *CoRR*, abs/2405.07992, 2024. 1, 2
- [34] Shuangfei Zhai, Navdeep Jaitly, Jason Ramapuram, Dan Busbridge, Tatiana Likhomanenko, Joseph Y. Cheng, Walter Talbott, Chen Huang, Hanlin Goh, and Joshua M. Susskind. Position prediction as an effective pretraining strategy. In *ICML 2022*, pages 26010–26027, 2022. 3
- [35] Lianghai Zhu, Bencheng Liao, Qian Zhang, Xinlong Wang, Wenyu Liu, and Xinggang Wang. Vision mamba: Efficient visual representation learning with bidirectional state space model. In *ICML 2024*, 2024. 1, 2, 3, 8